波 谱 学 杂 志
第 16 卷第 1 期 Vol. 16 No. 1
1999 年 2 月 Chinese Journal of Magnetic Resonance Feb. 1999

P-TYPE GRADIENT-ENHANCED DQF-COSY EXPERIMENTS SHOW LOWER t_1 NOISE THAN N-TYPE *

Lin Guoxing, Liao Xinli, Lin Donghai, Zheng Shaokuan
Chen Zhong and Wu Qinyi
(Department of Chemistry, Xiamen University, Xiamen 361005)

Abstract t_1 noise, stemming from the instabilities of pulse phases in 2D spectroscopy, has been investigated theoretically as well as experimentally. Based on the angular momentum operator I_x, I_y, I_z formalism, our deductions show that the different precessing directions of the magnetization between P-type and N-type gradient-enhanced DQF-COSY experiments result in that P-type gradient-enhanced DQF-COSY experiments refocus the phase errors of pulses, while N-type gradient-enhanced DQF-COSY experiments strengthen the effect of the phase errors of pulses. Therefore, t_1 noise in P-type gradient-enhanced DQF-COSY experiments is lower than that in N-type. In addition, the theoretical ratio of P-type to N-type is $\sqrt{3}:\sqrt{11}$, which is supported by our experimental results.

Key words NMR, DQF-COSY, PFG, Product operator, t_1 noise

1 INTRODUCTION

Since the introduction of pulse field gradients (PFG) to 2D NMR, there is a choice that we need to make between P-type (or anti-echo) coherence transfer pathway and N-type (or echo) pathway in the absolute value mode PFG experiment. The N-type pathway refocuses the effects of field inhomogeneity, and hence the signal intensity of N-type is higher than that of P-type, but the P-type pathway can reduce the signal of solvent and of small molecular impurities because they have longer spin-spin relaxation time[1,2]. Therefore when the shimming is excellent, both pathways give good results. In the absolute value COSY and

Received 21 Sep. 1998 Revised 3 Dec. 1998
*This project was supported by the National Natural Science Foundation of China(19605004) and State Key Laboratory for Physical Chemistry of the Solid Surface
林国兴, 男, 1971 年出生, 博士研究生

other sequences, they are nowadays used arbitrarily interchangeably. In the past, it was often regarded that there are no many differences between P-type and N-type experiments. However, Timothy J. Horne and Gareth A. Morris recently show that in gradient-enhanced COSY experiments, the ratio of t_1 noise in P-type to t_1 noise in N-type is $1:\sqrt{5}$ and t_1 noise in phase-cycled COSY is only a little worse than that in N-type COSY[1]. Their results are interesting and important, which urges us to make further study on the inherent differences in P-type and N-type gradient methods.

The double-quantum-filtered COSY (DQF-COSY) experiment is one of the most useful versions of the homonuclear correlation spectroscopy experiments[3-5]. It allows purging of spectra and simplifies the cross-peak multiple patterns. In the gradient methods, the coherence transfer pathway can be easily determined by shift operators I^+ and I^-, but it is not convenient for us to describe the whole evolution. In this paper we use the angular momentum operators I_x, I_y, I_z[6] to deduce the evolution of density operator in the DQF-COSY, because the angular momentum operators not only can describe the whole evolution of the pulse sequences, but also can take into account the effect of the phase errors of the pulses on the evolution. Based on the evolution results, we show that the t_1 noises caused by the instabilities of pulse phases in P-type and N-type are different. The P-type DQF-COSY shows lower t_1 noise than that of N-type DQF-COSY.

2 THEORY

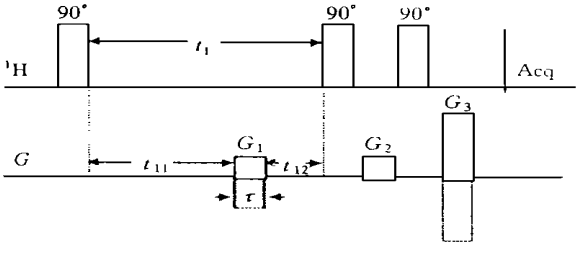

Fig. 1 Pulse sequence for the gradient enhanced DQF-COSY experiment

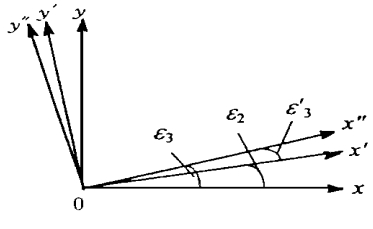

Fig. 2 Transformation of different coordinates

Consider the effect of changes of pulse phases on the t_1 noise of DQF-COSY sequence. Fig. 1 shows the Pulse sequence for the gradient-enhanced DQF-COSY experiment, which may be used for P-type or N-type gradient-enhanced absolute value DQF-COSY experiment depending on the magnitudes and signs of the three field gradient pulses used. The three field gradient pulses are of equal durations τ. The relation between G_1 and G_2 is $G_2 = \pm 3G_1$. The same sign is for N-type pathway selection and the opposite sign for the P-type selection. Let us arbitrarily set the receiver reference phase at zero and let the phases of the three pulses be fixed as $\varepsilon_1 + \Phi$, $\varepsilon_2 + \Phi$ and ε_3 respectively, where Φ is an arbitrary phase shift (which in practice will normally be a multiple of 90°) and ε_1, ε_2, ε_3 are small phase errors. We will describe the evolution of the density operator of a two-spin system by the angular momentum

operators I_x, I_y, I_z[6]. We may set the phase shift Φ at zero without loss of generality in the description. The two-spin system initially is assumed at thermal equilibrium in state I_{kz} and I_{lz}. After the first 90°_x pulse, the density operator of the two-spin system can be written as

$$\sigma_1 = I_{kx}\sin\varepsilon_1 - I_{ky}\cos\varepsilon_1 + I_{lx}\sin\varepsilon_1 - I_{ly}\cos\varepsilon_1 \tag{1}$$

Because k spin and l spin are actually at equivalent position, we may merely present the evolution of k spin for the simplicity. So Eq.[1] can be written as

$$\sigma_1 = I_{kx}\sin\varepsilon_1 - I_{ky}\cos\varepsilon_1 \tag{2}$$

In the course of the evolution period t_1, we may separate it into three intervals t_{11}, τ and t_{12} (see Fig. 1), $t_{11}+\tau+t_{12}=t_1$. In t_{11} and t_{12}, the spin system freely evolves under the influence the Hamiltonian $H = \sum_k \omega_k I_{kz} + 2\pi\sum_k\sum_l J_{kl} I_{kz} I_{lz}$. In τ, the spin system evolves under the Hamiltonian H and the pulsed field gradient. Therefore σ_1 evolves according to

$$\sigma_1 \xrightarrow{Ht_{11}} \xrightarrow{(H-\gamma G_i z I_z)\tau} \xrightarrow{Ht_{12}} \sigma_2 \tag{3}$$

Since H commutes with $-\gamma G_i z I_z$, Eq.[3] may be written as

$$\sigma_1 \xrightarrow{Ht_1} \xrightarrow{-\gamma G_i z I_z \tau} \sigma_2 \tag{4}$$

$$\begin{aligned}\sigma_2 = {} & [I_{kx}\sin(\omega_k t_1 + \varepsilon_1 + \theta_1) - I_{ky}\cos(\omega_k t_1 + \varepsilon_1 + \theta_1)]\cos\pi J_{kl} t_1 \\ & + [2I_{kx}I_{lz}\cos(\omega_k t_1 + \varepsilon_1 + \theta_1) + 2I_{ky}I_{lz}\sin(\omega_k t_1 + \varepsilon_1 + \theta_1)]\sin\pi J_{kl} t_1\end{aligned} \tag{5}$$

where θ_1 is the rotation angle of k spin and l spin caused by the first PFG pulse. The second 90°_x pulse will purge all components of σ_2 that are not in phase with it, giving out

$$\begin{aligned}\sigma_3 = {} & [I_{kx'}\sin(\omega_k t_1 + \varepsilon_1 + \theta_1 - \varepsilon_2) - I_{kz}\cos(\omega_k t_1 + \varepsilon_1 + \theta_1 - \varepsilon_2)]\cos\pi J_{kl} t_1 \\ & - [2I_{kx'}I_{ly'}\cos(\omega_k t_1 + \varepsilon_1 + \theta_1 - \varepsilon_2) + 2I_{kz}I_{ly'}\sin(\omega_k t_1 + \varepsilon_1 + \theta_1 - \varepsilon_2)]\sin\pi J_{kl} t_1\end{aligned} \tag{6}$$

where $I_{kx'}$ is the operator in a new coordinate. The relationship between the original coordinate and the new coordinate is sown in Fig. 2. For the convenience, we will replace $\omega_k t_1 + \varepsilon_1 + \theta_1 - \varepsilon_2$ with α. After the second PFG pulse, we obtain

$$\begin{aligned}\sigma_4 = {} & [(I_{kx'}\cos\theta_2 + I_{ky'}\sin\theta_2)\sin\alpha - I_{kz}\cos\alpha]\cos\pi J_{kl} t_1 \\ & - [2(I_{kx'}\cos\theta_2 + I_{ky'}\sin\theta_2)(I_{ly'}\cos\theta_2 - I_{lx'}\sin\theta_2)\cos\alpha \\ & + 2I_{kz}(I_{ly'}\cos\theta_2 - I_{lx'}\sin\theta_2)\sin\alpha]\sin\pi J_{kl} t_1\end{aligned} \tag{7}$$

The third 90°_x pulse will purge all components of σ_4 that are not in phase with it, giving

$$\begin{aligned}\sigma_5 = {} & [(I_{kx''}\cos\beta + I_{kz}\sin\beta)\sin\alpha + I_{ky''}\cos\alpha]\cos\pi J_{kl} t_1 \\ & - [2(I_{kx''}\cos\beta + I_{kz}\sin\beta)(I_{lz}\cos\beta - I_{lx''}\sin\beta)\cos\alpha \\ & - 2I_{ky''}(I_{lz}\cos\beta - I_{lx''}\sin\beta)\sin\alpha]\sin\pi J_{kl} t_1\end{aligned} \tag{8}$$

where $I_{kx''}$, $I_{ky''}$ belong to another coordinate shown in Fig. 2. Also, for the convenience, we substitute β for $\theta_2 - \varepsilon_3'$, $\varepsilon_3' = \varepsilon_3 - \varepsilon_2$. After the third PFG pulse, the density operator is

$$\begin{aligned}\sigma_6 = {} & \{[(I_{kx''}\cos\pm 3\theta + I_{ky''}\sin\pm 3\theta)\cos\beta + I_{kz}\sin\beta]\sin\alpha + (I_{ky''}\cos\beta \pm 3\theta - I_{kx''}\cos \\ & \pm 3\theta)\cos\alpha\}\cos\pi J_{kl} t_1 - \{2[(I_{kx''}\cos\pm 3\theta + I_{ky''}\sin\pm 3\theta)\cos\beta + I_{kz}\sin\beta][I_{lz}\cos\beta \\ & - (I_{lx''}\cos\pm 3\theta + I_{ly''}\sin\pm 3\theta)\sin\beta]\cos\alpha - 2(I_{ky''}\cos\pm 3\theta - I_{kx''}\cos\pm 3\theta)[I_{lz}\cos\beta \\ & - (I_{lx''}\cos\pm 3\theta + I_{ly''}\sin\pm 3\theta)\sin\beta]\sin\alpha\}\sin\pi J_{kl} t_1\end{aligned} \tag{9}$$

where, $+3\theta$ for N-type pathway, -3θ for P-type pathway. When we perform spatial integral, those terms that will survive are

$$\sigma_7 = I_{kz}\sin\beta\sin\alpha\cos\pi J_{kl}t_1 - [2(I_{kx}''\cos\pm 3\theta + I_{ky}''\sin\pm 3\theta)\cos\beta I_{lz}\cos\beta - 2I_{kz}\sin\beta(I_{lx}''\cos\pm 3\theta + I_{ly}''\sin\pm 3\theta)\sin\beta]\cos\alpha\sin\pi J_{kl}t_1 \quad (10)$$

For P-type pathway, after performing spatial integral, we get the observable operator

$$\sigma_{obs} = -2\times\frac{1}{8}[I_{kx}''I_{lz}\cos(-2\varepsilon_3' + \varepsilon_1 - \varepsilon_2 + \omega_k t_1) + I_{ky}''I_{lz}\sin(-2\varepsilon_3' + \varepsilon_1 - \varepsilon_2 + \omega_k t_1) + I_{kz}I_{lx}''\cos(-2\varepsilon_3' + \varepsilon_1 - \varepsilon_2 + \omega_k t_1) + I_{kz}I_{ly}''\sin(-2\varepsilon_3' + \varepsilon_1 - \varepsilon_2 + \omega_k t_1)]\sin\pi J_{kl}t_1 \quad (11)$$

Transforming I_{kx}'', I_{ky}'' to x', y' coordinate, then to x, y coordinate, we obtain

$$\sigma_{obs} = -2\times\frac{1}{8}[I_{kx}''I_{lz}\cos(-\varepsilon_3' + \varepsilon_1 + \omega_k t_1) + I_{ky}''I_{lz}\sin(-\varepsilon_3' + \varepsilon_1 + \omega_k t_1) + I_{kz}I_{lx}''\cos(-\varepsilon_3' + \varepsilon_1 + \omega_k t_1) + I_{kz}I_{ly}''\sin(-\varepsilon_3' + \varepsilon_1 + \omega_k t_1)]\sin\pi J_{kl}t_1 \quad (12)$$

where $-\varepsilon_3' + \varepsilon_1 = -\varepsilon_3 + \varepsilon_2 + \varepsilon_1$.

For N-type pathway, after performing spatial integral, we get the observable operator

$$\sigma_{obs} = -2\times\frac{1}{8}[I_{kx}''I_{lz}\cos(-2\varepsilon_3' + \varepsilon_1 - \varepsilon_2 + \omega_k t_1) - I_{ky}''I_{lz}\sin(-2\varepsilon_3' + \varepsilon_1 - \varepsilon_2 + \omega_k t_1) + I_{kz}I_{lx}''\cos(-2\varepsilon_3' + \varepsilon_1 - \varepsilon_2 + \omega_k t_1) - I_{kz}I_{ly}''\sin(-2\varepsilon_3' + \varepsilon_1 - \varepsilon_2 + \omega_k t_1)]\sin\pi J_{kl}t_1 \quad (13)$$

Transforming I_{kx}'', I_{ky}'' to coordinate x', y', then to coordinate x, y, we obtain

$$\sigma_{obs} = -2\times\frac{1}{8}\{I_{kx}''I_{lz}\cos(-3\varepsilon_3' - 2\varepsilon_2 + \varepsilon_1 + \omega_k t_1) + I_{ky}''I_{lz}\sin[-(-3\varepsilon_3' - 2\varepsilon_2 + \varepsilon_1 + \omega_k t)] + I_{kz}I_{lx}''\cos(-3\varepsilon_3' - 2\varepsilon_2 + \varepsilon_1 + \omega_k t_1) + I_{kz}I_{ly}''\sin[-(-3\varepsilon_3' - 2\varepsilon_2 + \varepsilon_1 + \omega_k t)]\}\sin\pi J_{kl}t \quad (14)$$

where $-(-3\varepsilon_3' - 2\varepsilon_2 + \varepsilon_1) = -(-3\varepsilon_3 + \varepsilon_2 + \varepsilon_1)$.

According to Parseval's theorem[1], the integrated noise power in the f_1 dimension of the final 2D spectrum will be the same as that in the t_1 time domain. Therefore the t_1 noise in an absolute value mode spectrum will be proportional to the square root of the sum of the squares of the error contributions. If the phase errors ε_1、ε_2 and ε_3 are all uncorrelated and equal root mean square error signal amplitude ε, in the P-type pathway and N-type pathway, the ratios N/S of the root mean square error signal amplitudes to the moduli of the signals will be

$$(N/S)^p = \sqrt{(-\varepsilon)^2 + \varepsilon^2 + \varepsilon^2} = \sqrt{3}\varepsilon \quad (15)$$

and

$$(N/S)^n = \sqrt{(-3\varepsilon)^2 + \varepsilon^2 + \varepsilon^2} = \sqrt{11}\varepsilon \quad (16)$$

therefore the ratio of t_1 nose in P-type pathway to t_1 noise in N-type pathway is

$$(N/S)^p : (N/S)^n = \sqrt{3} : \sqrt{11} \quad (17)$$

3 EXPERIMENT

We recorded the proton absolute value mode DQF-COSY experiments on a Varian Unity 500 spectrometer, using a 5mm triple resonance pulsed field gradient probe. The sample used is triphenylphosphate in deuterochloroform. The spectral width was set to 2192 Hz in each dimension, with 1024 complex data points in t_2 (acquisition time 0.234s) and 512 t_1 increments. The recycle time was 8.6s. Gradient enhanced DQF-COSY were carried out using four scans per increment with rectangular gradient pulses of 2.5ms duration and approximately 6×10^{-4}T cm^{-1} for G_1 srength. The absolute value spectra were obtained by one time zero-filling in t_1 and sine-bell weighting centered on 0.117s in t_1 and 0.117s in t_2.

4 RESULTS

The full absolute value gradient-enhanced DQF-COSY spectra of P-type and N-type obtained are shown in Fig. 3. Fig. 4 shows the expansions of the regions of the DQF-COSY spectra between 7.60ppm and 7.80ppm in f_2 dimension. The f_1 cross-sections through the DQF-COSY spectra at $f_2 = 7.728$ppm are shown on the top of Fig. 4. All the figures use the same horizontal, vertical and intensity scales for display. From Fig. 4, it can be seen clearly that the level of t_1 noise in P-type is lower than N-type. The integrated peak values, integrated t_1 noise values, signal to root mean square noise ratios and peak integral to t_1 noise integral of the absolute value f_1 cross-sections in the 2D spectra are shown in Tab. 1, together with their relative ratios.

Tab. 1　Peak integral intensities, t_1 noise integral intensities, signal to t_1 noise ratios and peak integral to t_1 noise integral ratio for f_1 cross-sections through absolute value mode gradient-enhanced DQF-COSY spectra

	Case 1		Case 2	
	P-type	N-type	P-type	N-type
f_1 cross-sections position in 2D spectra, namely f_2 frequency (ppm)	7.728		7.862	
Peak integral region(ppm)	8.5~9.5		8.5~9.5	
t_1 noise integral region and sampling region(ppm)	7.0~8.0		7.0~8.0	
Peak integral values (arbitrary units)	928.11	1762.52	730.21	674.85
t_1 noise integral values (arbitrary units)	9.12	33.16	14.76	11.20
Signal to noise ratio (arbitrary units)	1408.3	966.1	1018.9	860.2
Noise to signal ratio relative to P-type	1	1.46	1	1.18
Peak integral to t_1 noise integral ratio (arbitrary units)	101.76	53.15	60.25	49.56
t_1 noise integral to peak integral ratio relative to P-type	1	1.92	1	1.22

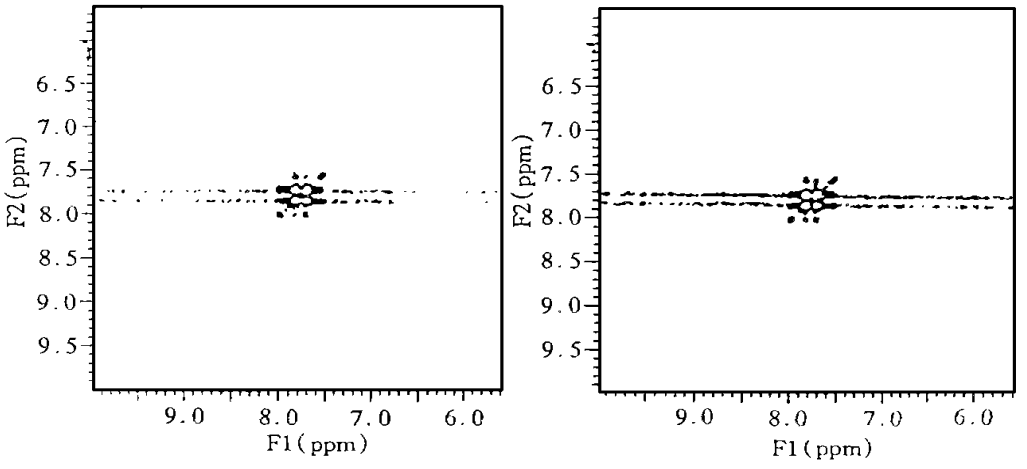

Fig. 3 P-type gradient-enhanced DQF-COSY spectrum (left) and N-type spectrum(right)

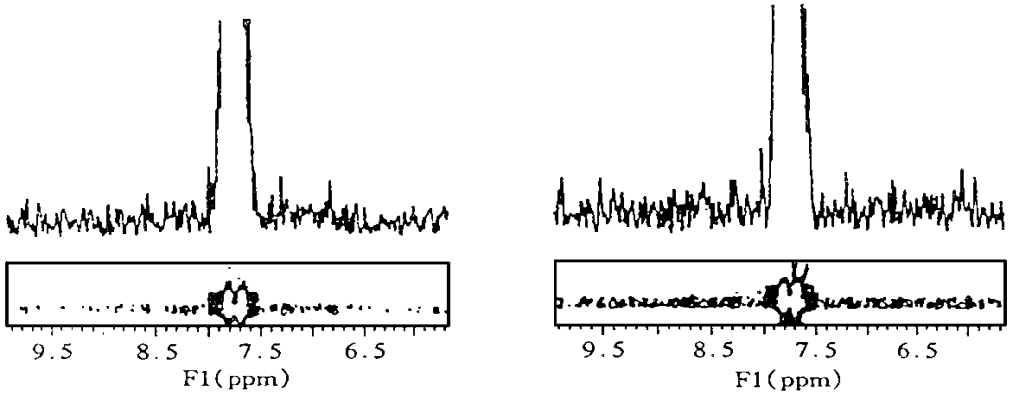

Fig. 4 f_1 cross-sections through and expansions of the 2D spectra (See Fig. 3)

From Tab. 1, we see that the ratios in the frequency ($f_2 = 7.728$ppm) near the transmitter frequency are higher than those in the frequency ($f_2 = 7.862$ppm) that is off resonance. We will make further study on this problem why the ratios are higher than others when the frequency is on resonance. From the ratios in Tab. 1, we see clearly that t_1 noise in N-type is greater than that in P-type.

5 DISCUSSION

As the foregoing analysis and the experimental results presented, t_1 noise in N-type absolute value mode gradient enhanced DQF-COSY experiments is greater than that of P-type. Our results are similar to those obtained by Gareth A. Morris etc. who showed that in gradient enhanced COSY experiments, the ratio of t_1 noise in P-type to t_1 noise in N-type is $1:\sqrt{5}$. Our theoretical ratio of t_1 noise in P-type to t_1 noise in N-type in DQF-COSY is $\sqrt{3}:\sqrt{11} \approx 1:1.91$. In our experiment, the t_1 noise of P-type is lower than that of N-type. The largest t_1 noise ratio of P-type to N-type is 1 :1.46. It is reasonable that in our experiment the ratios of P-type to N-type are lower than the theoretical values because there are many sources of t_1

noise, such as phase, frequency, gain or shimming irreproducibility.

The result presented here is important in cases when signals are strong enough that t_1 noise will be the limiting factor in detection of cross peaks. For example, in the intermolecular multiple quantum coherences (IMQC) experiments[7,8], the solvent-solute peak may be covered by t_1 noise of solvent signal when the concentration of solute is very low. In gradient-enhanced DQF-COSY experiment, when the third 90°_x pulse keeps all $I_{kx''}$、$I_{lx''}$ magnetizations of the different portions of the sample in a plane through z-axis (namely x'', z plane in coordinate) and rotates all magnetizations in z-direction into -y''-direction (in y'', z plane), all the observable magnetizations in the x'', z plane have acquired total $-2\varepsilon_3' - \varepsilon_2 + \varepsilon_1$ phase errors in the evolution. In the P-type pathway, after the third PFG, the magnetizations spread spirally over the whole sample and the spatial integral of magnetizations precesses through $-2\varepsilon_3' - \varepsilon_2 + \varepsilon_1$ angle. Seen from the x, y coordinate, the $(-2\varepsilon_3' - \varepsilon_2 + \varepsilon_1)$ angle must be added by angle $(\varepsilon_3' + \varepsilon_2)$ between x, y coordinate and x'', y'' coordinate, So the P-type phase error is $(-\varepsilon_3' + \varepsilon_1) = (-\varepsilon_3 + \varepsilon_2 + \varepsilon_1)$. In N-type pathway, the spatial integral of magnetizations precesses through $-(-2\varepsilon_3' - \varepsilon_2 + \varepsilon_1)$ angle. Added by angle $(\varepsilon_3' + \varepsilon_2)$, it becomes $-(-3\varepsilon_3' - 2\varepsilon_2' + \varepsilon_1)$. So the N-type phase error is $-3\varepsilon_3' - 2\varepsilon_2' + \varepsilon_1 = -3\varepsilon_3 + \varepsilon_2 + \varepsilon_1$. In gradient-enhanced HMQC experiment, though the spatial integrals of magnetizations precess in different directions in P-type and N-type pathway, there are equivalent t_1 noise levels in P-type and N-type pathway because the dephasing angle and refocusing angle are finished by different spins such as ^1H、^{13}C and the different precessing angles are seen from x, y coordinate directly. In gradient-enhanced NOESY experiment, in the mixing period, the PFG pulse does not affect the magnetization in z-direction, so the phase error will not appears in the rotation angle caused by the PFG pulse in mixing period thus there are no different t_1 noise levels in P-type and N-type pathway. When the phase error of the pulse appears in magnetizations in the same planes such as x', z plane or x'', z plane, the integrals of the magnetizaions precess into different directions, which will result in different t_1 noise levels in P-type pathway and N-type pathway seen from the x, y coordinate.

References

1 Timothy J. Horne, Gareth A. Morris. Magn Reson in Chem, 1997, 35: 680—686

2 Bax A, Freeman R, Morris G A. J Magn Reson, 1981, 42: 164

3 Hurd R E. J Magn Reson, 1990, 87: 422—428

4 James Keeler, Clowes R T, Davis A L, Laue E D. Method in Enzymology, 1994, 239: 145—207

5 Anthony A. Shaw, Christophe Salaun, Jean-Francois, Dauphin, Bernard Ancian, J Magn Reson, 1996, 120: 110—115

6 Sorensen O W, Eich G W, Levitt M H, Bodenhausen G, Ernst R R. Progress in NMR Spectroscopy, 1983, 16: 163—192

7 Warren S. Warren, Wolfgang Richter, Amy Hamilton Andreotti, Bennett T. Farmer Ⅱ. Science, 1993, 262(24): 2005—2009

8 He Qiuhong, Wolfgang Richter, Sujatha Vathyam, Warren S. Warren. J Chem Phys, 1993, 98(9): 6779—6800

脉冲梯度场增强的 DQF-COSY 实验 t_1 噪声研究

林国兴, 廖新丽, 林东海, 郑绍宽[a], 陈忠, 吴钦义
(厦门大学化学系, [a] 厦门大学物理系, 厦门 361005)

摘 要

脉冲相位的不稳定性是导致二维谱中的 t_1 噪声的原因之一. 本文从理论上和实验上对脉冲相位不稳定性所引起的 t_1 噪声进行了研究. 从角动量算符 I_x, I_y 和 I_z 推导中发现, 由于磁化矢量在 P 型和 N 型 DQF-COSY 实验的脉冲梯度场中进动方向的内在差异, 一部分脉冲相位误差在 P 型 DQF-COSY 实验会被重聚掉, 在 N 型 DQF-COSY 实验中却会被加重. 因此 P 型 DQF-COSY 实验的 t_1 噪声比 N 型小. 理论推导还得到 t_1 噪声在 P 型和 N 型中的理论比值为 $\sqrt{3}:\sqrt{11}$. 以上理论结果得到我们实验结果的支持.

关键词 NMR, DQF-COSY, 脉冲梯度场, t_1 噪声, 积算符